Analyst

Cite this: *Analyst*, 2012, **137**, 3452

www.rsc.org/analyst

PAPER

Dissociated neuronal culture expressing ionotropic odorant receptors as a hybrid odorant biosensor—proof-of-concept study

Norio Tanada,[a] Takeshi Sakurai,[a] Hidefumi Mitsuno,[a] Douglas J. Bakkum,[ab] Ryohei Kanzaki[ac] and Hirokazu Takahashi*[acd]

Received 12th January 2012, Accepted 12th June 2012
DOI: 10.1039/c2an35058k

Artificial odorant sensors generally perform poorer than olfactory systems in living organisms. The excellent performances of living odorant systems are achieved by the molecular recognition abilities of odorant receptors and the neuronal information processing that follows. To take advantages of this, here we propose a novel hybrid odorant biosensor by means of expressing ionotropic odorant receptors of insects into dissociated neuronal cultures of rodents. This combination of materials brings significant advantages such as easy functional expression, prolonged lifetime, and an ability to amplify the weak ionic currents of odorant receptors. In the present work, pheromone receptors and co-receptors of silkmoth, *i.e.*, BmOR1 and BmorOrco, were expressed in neuronal cultures *via* liposome transfection. Consequently, BmOR1 and BmorOrco were co-expressed in 8% of neuronal cells, and both receptors were co-localized on a cell membrane. In Ca++ imaging experiments, synchronous increase of calcium signals at the presentation of BOL was found in both transfected cells and non-transfected cells in a dose-dependent manner. These results provide the proof-of-concept of the proposed hybrid odorant biosensor.

Introduction

Physico-chemical techniques, such as metal-oxide semiconductors, intrinsically conducting polymers, quartz crystal microbalances, surface plasmon resonators, *etc.*, have been extensively utilized to develop artificial odorant sensors. These conventional odorant sensors, however, generally perform more poorly than olfactory systems in living organisms in terms of sensitivity, selectivity and variety of detectable odorants. In addition, for reliable detections of odorants, often real-time detection is sacrificed. The excellent performances of living odorant systems are achieved by the molecular recognition abilities of odorant receptors and the neuronal information processing that follows.

In some pioneering works, natural living systems were used as essential components of odorant sensors; *e.g.*, an intact olfactory epithelium,[1] HEK-293 cells expressing vertebrate odorant receptor,[2] *Xenopus laevis oocytes* expressing insect odorant receptors,[3] *etc.*[4–6] These hybrid biosensors, however, have an inevitably short functional period because the lifetime of the living cells used is limited up to a few days. Furthermore, the reaction time is much longer than in the original olfactory systems possibly because non-linear amplification by neural systems is not effective.

In order to overcome these shortcomings, here we propose a novel hybrid biosensor utilizing ion channels with built-in odorant receptors from insects combined with dissociated cultures of neurons of rats. This combination of materials has significant potential advantages. First, the ion channel's built-in structure of insect odorant receptor allows functional expression in target cells much easier than G-protein coupled receptors (GPCRs), which are commonly present in vertebrate olfactory systems. For example, pheromone receptors of the silkmoth, *Bombyx mori*, used in this study, forms heteromeric complexes with a co-receptor, serving as a non-selective cationic channel.[7] Thus, unlike GPCRs, reconstruction of intracellular signaling cascades originating in such receptors is not needed. Second, because significant populations of neurons do not turn over throughout the lifespan of an individual organism,[8] they could provide a significantly longer functional period as a sensor than would be possible with non-neuronal cells. Third, neurons could non-linearly amplify weak ionic currents of odorant receptors into easily detectable action potentials, enabling real-time detection. Fourth, through synaptic connections, odorant-evoked activities could be amplified as distinct neuronal activity patterns in the culture. Thus, individual neurons expressing odorant receptors and neuronal culture would serve as pre- and main-amplifiers, respectively.

[a]*Research Center for Advanced Science and Technology, The University of Tokyo, Komaba 4-6-1, Meguro-ku, Tokyo 153-8904, Japan. E-mail: takahashi@i.u-tokyo.ac.jp; Fax: +81-3-5452-5196; Tel: +81-3-5452-5196*
[b]*Department of Biosystems Science and Engineering, ETH Zurich, Basel, Switzerland*
[c]*Graduate School of Information Science and Technology, The University of Tokyo, Hongo 7-3-1, Bunkyo-ku, Tokyo 113-8656, Japan*
[d]*PRESTO, JST, 4-1-8 Honcho, Kawaguchi, Saitama, 332-0012, Japan*

In the present study, we provide the proof-of-concept for this proposed odorant sensor in terms of functional consequences that odorant-evoked signals of transfected receptors can be promptly amplified as network-wide activity patterns in the culture. The silkmoth odorant receptors were expressed in dissociated neuronal cultures of rats through liposome transfection.[9] Then, the expression and transfection efficiency were comprehensively evaluated through confocal observation, reverse transcript PCR (RT-PCR) and immunocytochemistry. Lastly, Ca++ imaging demonstrated that the odorant receptors functioned and the odor-evoked signals were amplified into spatio-temporal activity patterns in the neuronal culture.

Materials and method

Experimental setup

Fig. 1(a) depicts a schematic diagram of the experimental setup that we have developed and used in the present work. In neuron-glia coculture, odor-sensitive neurons were sparsely derived by means of liposome co-transfection of BmOR1, the gene encoding the odorant receptor for the major sex pheromone bombykol,[10,11] and BmorOrco (odorant receptor co-receptor).[12,13] As shown in Fig. 1(b), BmOR1 and BmorOrco form a heteromeric complex, which serves as a non-selective cationic channel selectively responding to pheromone substance, bombykol (BOL). The pheromone substance and other chemicals were administered to neuronal cells through the tip of a glass micropipet with a 2 μm diameter by manually applying pressure. An upright fluorescence microscope (BX51WI, Olympus) or an inverted microscope (Zeiss, Axiovert S100) were used to observe test samples and measure Ca++ signals in the culture.

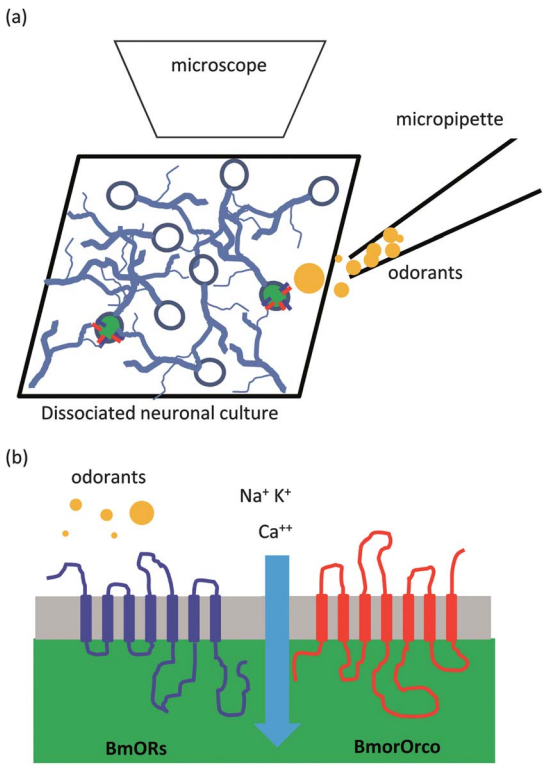

Fig. 1 Odorant biosensor using a dissociated neuronal culture expressing ionotropic odorant receptors. (a) Experimental setup. Some neurons (filled) in a dissociated culture have odorant receptors expressed. Odorants are administrated to the neuronal culture through the tip of micropipette. (b) Ionotropic odorant receptor used in the present study. A pheromone receptor of silkmoth and co-receptor, BmOR1 and BmorOrco, form a heteromer serving as a non-selective cationic channel.

Cell culture

All procedures were approved by our institutional committee in the University of Tokyo and performed in accordance with "Guiding Principles for the Care and Use of Animals in the Field of Physiological Science" of the Japanese Physiological Society.

Neuron-glia coculture was prepared from the cerebral cortex of E18 (embryonic 18 day-old) Wistar rat.[14–16] Trypsin (Gibco, 15050-065)-dissociated cells were plated and incubated on poly-L-lysine- and laminin-coated multi-well plates (Sumitomo Bakelite Co. Ltd., MS-0024L or MS-0035L). The culture medium consisted of neurobasal (Gibco, 21103-049) with 0.5 mM L-glutamine and 2% B-27 supplement (Gibco, 17504-044). In each preparation, the number of cells plated within a 300 μl droplet was approximately 300 000 to investigate transfection efficiency and 30 000 for Ca++ imaging experiments. Sparser cultures of 30 000 cells were used for Ca++ imaging so that activities of individual neurons within a visual field were easily identified. Half of the growth medium was exchanged twice a week. These cultures were placed in an incubator at 37 °C with H_2O-saturated atmosphere, consisting of 95% air and 5% CO_2.

Construction of DNA vectors

The EGFP coding region lacking a stop codon was amplified from pEF-EGFP[17] by PCR using the following specific primers with EcoRI (forward) and NotI (reverse) restriction sites (forward, 5′-CCAGAATTCGCCACCATGGTGAGCAAGGG-3′ and reverse, 5′-CGGGCGGCCGCCTTGTACAGCTCGTC CAT-3′). The amplified fragment was digested with EcoRI and NotI, and subcloned into corresponding sites of pEF-EGFP to replace EGFP containing a stop codon with that lacking a stop codon. Then, the coding sequence of BmOR1 and BmorOrco was PCR-amplified, digested with NotI (forward) and XbaI (reverse) restriction sites (for BmOR1, forward, 5′-ATG GCGGCCGCCATGTTACTATCCTTCAA-3′ and reverse 5′-GGCTCTAGA TTATGTTGCCACCGTTCGAA-3′; for BmorOrco, forward, 5′-ATGGCGGCCGCCATGATGAC CAAGGTCAAG-3′ and reverse 5′-GGCTCTAGA CTACTT CAGTTGGATCAACA-3′) and subcloned into a corresponding site of the resultant vector to create pEF-EGFP-BmOR1 and pEF-EGFP-BmorOrco, which were designed to express the N-terminal EGFP-fused BmOR1 and BmorOrco, respectively. The DsRED coding region lacking a stop codon was amplified from pCMV-DsRed-Express Vector (Takara, 632416) by PCR using the following specific primers with EcoRI (forward) and NotI (reverse) restriction sites (forward, 5′CAAGAATTCGCCACC ATGGACAACACCGA-3′ and reverse, 5′-ATAGCGGCCGCC TGGGAGCCGGAGTGGCG-3′). The amplified fragment was digested with EcoRI and NotI, and subcloned into corresponding sites of pEF-EGFP to replace DsRED containing a stop codon with that lacking a stop codon. Then, the coding sequence

of BmOR1 and BmorOrco was PCR-amplified, digested as described before and subcloned into a corresponding site of the resultant vector to create pEF-DsRED-BmorOrco, which were designed to express the N-terminal DsRED-fused BmorOrco.

To generate pEF-BmOR1 and pEF-BmorOrco, the coding region of BmOR1 and BmorOrco was PCR-amplified using the following specific primers with KpnI (forward) and XbaI (reverse) restriction sites (for BmOR1, forward, 5′-GGCGGTA CCGCCACC ATGTTACTATCCTT-3′ and reverse 5′-GGCTC TAGATTATGTTGCCACCGTTCGAA-3′; for BmorOrco, forward, 5′-AACGGTACCGCCACCATGATGACCAAGGT-3′ and reverse 5′-GGCTCTAGACTACTTCAGTTGGATCA ACA-3′). The amplified fragments were digested with KpnI and XbaI and subcloned into corresponding sites of pEF-EGFP. The resultant constructs were sequenced on an ABI310 genetic analyzer (Applied Biosystems) to verify correct amplification and insertion into the vectors.

Transfection

At 6 days *in vitro* (DIV), the neurobasal-based culture medium was replaced with minimum essential medium (MEM) (Gibco, 11095-080), 15 mM HEPES (Gibco, 15630-106), 0.45% glucose, 1 mM sodium pyruvate, and 2 mM L-glutamine. After incubation for 24 h, transfection was carried out using Lipofect-Amine2000 (Invitrogen, 11668-027) according to the manufacturer's instruction.

pEF-EGFP-BmOR1 and pEF-DsRED-BmorOrco were transfected either simultaneously or sequentially. For simultaneous co-transfection, lipofectamine medium containing pEF-EGFP-BmOR1 and pEF-DsRED-BmorOrco was added dropwise to neuronal cultures for a 30 min incubation. For sequential transfection, lipofectamine medium containing pEF-EGFP-BmOR1 was initially added dropwise to neuronal cultures for a 15 min incubation. This medium was then exchanged to pEF-DsRED-BmorOrco containing medium for another 15 min incubation.

For evaluation of these transfections, confocal imaging (LSM510, Zeiss) was first used to identify expression of the odorant receptors on a membrane of cell. Second, fluorescent microscopic observation with the help of immunocytochemistry evaluated the transfection efficiency. Third, RT-PCR investigated the expression of odorant receptors at the mRNA level. Lastly, Ca++ imaging tested odorant receptor functionality.

Immunocytochemistry

Three days after transfection, neuronal cells were fixed *in situ* by replacing growth medium with 4% paraformaldehyde. After fixing, the cells were washed with phosphate buffered saline (PBS), and permeablised with Triton-X-100 (0.25% solution in PBS) for 10 min, blocked with Block-Ace (4% solution in Triton-X-100 solution), followed by three PBS washes. Then, the cells were incubated with a primary antibody solution containing 1 : 500 mouse anti-NeuN IgG (Millipore, MAB377), 1 : 200 rabbit anti-GFP IgG (Invitrogen, A11122) for 1 day. NeuN is a neuron specific marker protein localized in the nucleus. After the antibody solution was washed off with PBS, the cells were incubated with a secondary antibody solution containing 1 : 200 anti-mouse Cy3-labeled IgG (Invitrogen, A10521) and 1 : 200 anti-rabbit Alexa488-labeled IgG (Invitrogen, A11034) for 2 h in the dark, followed by a PBS wash.

Quantification of transfection efficiency

To quantify the efficiency of transfection, the number of fluorescently labeled cells was counted. Through a modified GFP filter cube (Olympus, U-MWIB/GFP: excitation filter, BP460–495; dichroic mirror, DM505; emission filter, BA515–550), DsRed filter cube (Olympus, U-MWIY2/DsRED: excitation filter, BP545–580; dichroic mirror, DM600; emission filter, BA610IF) or Cy3 filter cube (Olympus, U-Cy3-4040-OMF: excitation filter, BP530–550; dichroic mirror, DM570; emission filter, BA575IF), a fluorescent image was acquired through an $\times 10$ object lens and photographed by either a digital camera (Sony, $\alpha 350$) on the inverted microscope with an exposure time of 2 s or cooled EM-CCD camera (Hamamatsu Photonics, C9100-02) on the upright microscope with an exposure time of 1 s. Two sets of 250 W metal halide lamps (Kiyohara Optics, KMH-250) were used to excite fluorescence.

The transfection efficiency was defined as the ratio of the number of anti-NueN and anti-EGFP positive cells [NeuN+, EGFP+] to the number of anti-NueN positive cells [NeuN+], *i.e.*, [NeuN+, EGFP+]/[NeuN+]. This efficiency was quantified in preparations with simultaneous co-transfection of pEF-EGFP-BmOR1 and pEF-BmorOrco (pEF-EGFP-BmOR1 + pEF-BmorOrco) and those with pEF-BmOR1 and pEF-EGFP-BmorOrco (pEF-BmOR1 + pEF-EGFP-BmorOrco).

Co-transfection efficiency was then estimated in preparations transfected with pEF-EGFP-BmOR1 and pEF-DsRED-BmorOrco. The co-transfection efficiency was defined as the ratio of the number of EGFP and DsRED positive cells [EGFP+, DsRED] to the total number of fluorescently labeled cells, *i.e.*, [EGFP+, DsRED]/{[EGFP+] + [DsRED+] − [EGFP+, DsRED]}.

For the estimation of these efficiencies, 4 culture dishes were investigated each with 4 separate visual fields of 0.4 mm × 0.4 mm (*i.e.*, $n = 16$).

RT-PCR

Total RNA was separately isolated from cells transfected with pEF-EGFP, with both pEF-BmOR1 and pEF-BmorOrco, and cells not transfected using RNeasy Plus Mini kit (QIAGEN, 74134), treated with DNaseI at 37 °C for 1 h, and heat treated at 80 °C for 10 min. RNA was reverse-transcribed using an oligo-dT adaptor primer (Takara, RNA PCR kit (AMV) ver3.0, RR019A) and avian myeloblastosis virus reverse transcriptase (Takara RNA PCR kit (AMV) ver3.0, RR019A) at 42 °C for 35 min. cDNA of the EGFP, BmOR1 and BmorOrco was amplified using Ex *Taq* DNA polymerase (Takara, RRo6A) and the primer pairs for EGFP (5′-ACGTAAACGGCCACAA GTTCAGCGTGTCC-3′,3′-CTTGTACAGCTCGTCCATGC CGAGAGTGA-5′), BmOR1 (5′-GGATTGGTAATGTTT GATTTGCTCATGTG-3′, 3′-TGTTGCCACCGTTCGAAG CATCACGAAAT-5′), and BmorOrco (5′-GACCGAGAAA GTACCAGATGCAGTAGATA-3′, 3′-CTTCAGTTGGAT CAACACCATGAAGTACG-5′) under the following thermal

program; 30 cycles of 94 °C for 1 min, 55 °C for 1 min and 72 °C for 1 min. Equal amounts of the PCR products were separated by electrophoresis on 1.0% agarose gels.

Ca++ imaging

At 10 DIV, to investigate the functional expression of odorant receptors, Ca++ imaging was used to test if pheromone substances effectively activated BmOR1 and BmorOrco-co-expressing cells. As a calcium indicator, 4 μM X-Rhod-1, AM (Invitrogen, X14210) was loaded to the culture for 20 min before imaging experiments. After the dye loading, the normal culture medium was replaced and used during Ca++ imaging. X-Rhod-1, AM was solubilized in 8 μl, 20% Pluronic F-127 in DMSO (AnaSpec, 84041), then sonicated and diluted in 10 ml balanced salt solution (BSS) to 4 μM. BSS had the following composition: NaCl, 119 mM; KCl, 2.5 mM; NaH_2PO_4, 1.0 mM; $CaCl_2$, 4 mM; $MgCl_2$ $6H_2O$, 4 mM; D-glucose, 11 mM.

Fluorescence images were observed through an upright fluorescence microscope with an ×10 objective lens (Olympus, UPlanF1) and captured with the cooled EM-CCD camera. The intensity of fluorescent light emission at 610 nm, under excitation at 510 nm, was monitored from each single X-Rhod-1 loaded cell. Camera acquisition rate was 1 s and Ca++ signals were measured for 90 s. Ca++ changes were obtained with HiPic 8.1.0 (Hamamatsu Photonics) and analyzed with custom-made Python codes. For the initial 30 s of each measurement, Ca++ signals were averaged to obtain the base line.

BOL was freshly prepared before experiments by diluting 1 M stock solution in DMSO with BSS solution to the appropriate concentration for each experiment. Odorants were administered to the target cells for 30 s through the tip of a microelectrode.

When blocking synaptic transmission, APV, CNQX and bicuculline methiodide (BMI) were added to external medium at 50, 10 and 100 μM, respectively.

Results

Transfection of BmOR1 and BmorOrco

Fig. 2(a) (i) and (ii) show fluorescence images of neuronal cultures co-transfected with pEF-EGFP-BmOR1 and pEP-DsRED-BmorOrco. The overlay image in Fig. 2(a) (iii) shows that the fluorescence pattern of EGFP almost matched the DsRED pattern, suggesting that BmOR1 and BmorOrco are highly likely to be co-expressed. Further direct confocal observations of a transfected cell in Fig. 2(b) (i)–(iii) confirmed the co-expression of BmOR1 and BmorOrco. In particular, these receptors were targeted onto the plasma membrane of the cell, where receptors can be functional.

Fig. 2(c) quantifies the transfection efficiency when BmOR1 and BmorOrco were simultaneously co-transfected: the efficiencies of BmOR1 and BmorOrco were approximately 8 and 12%, respectively, BmorOrco tending to have a higher efficiency than BmOR1. Fig. 2(d) quantifies the co-transfection ratio of BmOR1 and BmorOrco on the basis of the number of fluorescence-positive cells within a visual field of 0.4 mm × 0.4 mm. The co-transfection ratio was over 60% in simultaneous transfection [Fig. 2(d) (i)], while below 5% in sequential transfection [Fig. 2(d) (ii)]. Thus, simultaneous transfection was superior for

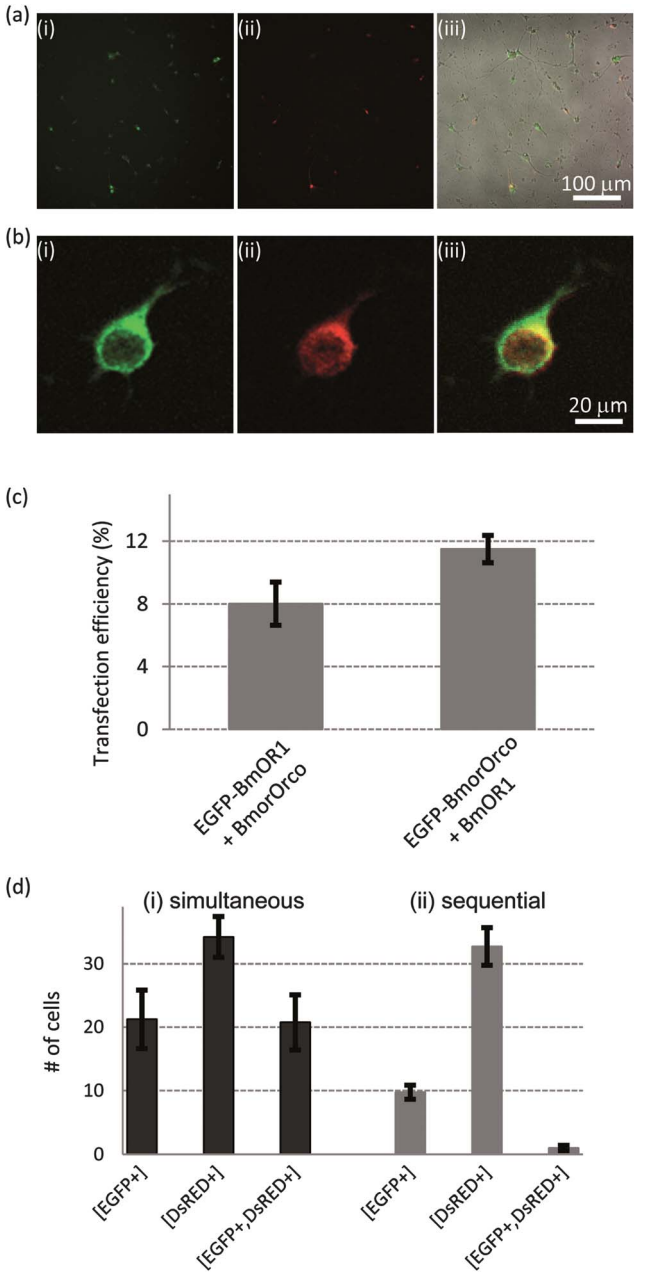

Fig. 2 Transfection of odorant receptors. (a) Fluorescent microscopic observation of a neuronal culture co-transfected with pEF-EGFP-BmOR1 and pEF-DsRED-BmorOrco constructs: (i) EGFP, (ii) DsRED and (iii) overlaid image. (b) Direct confocal observation of a living transfected neuronal cell with BmOR1 and BmorOrco targeted onto the plasma membrane. (c) Transfection efficiency of BmOR1 and BmorOrco. Transfection efficiency was defined as the ratio of EGFP positive cells to NueN positive cells. The efficiencies of BmOR1 and BmorOrco were evaluated by fluorescent images of BmOR1-EGFP fusion protein (EGFP-BmOR1 + BmorOrco) and BmorOrco-EGFP fusion protein (BmOR1 + EGFP-BmorOrco), respectively. Error bars indicate s.e. (d) The number of fluorescent cells within a visual field after (i) simultaneous and (ii) sequential co-transfections. The numbers of GFP-positive cells ([GFP+]), DsRED-positive cells ([DsRED+]) and double-positive cells ([EGFP+, DsRED+]) were quantified.

co-expressing BmOR1 and BmorOrco in the same cell with co-transfection ratio estimated at 8% of neuronal cells.

Ca++ imaging of transfected neuronal cultures in response to odorants

We next examined the responsiveness of cells expressing BmOR1 and BmorOrco to BOL. For this, we simultaneously co-transfected with pEF-EGFP, pEF-BmOR1, and pEF-BmorOrco to avoid possible deteriorative effects of N-terminal fused fluorescent protein on the function of BmOR1 and BmorOrco. In Fig. 3, RT-PCR experiments using primers specific for each gene showed that EGFP, BmOR1 and BmorOrco transcripts were detected in the transfected cells but not in non-transfected cells, confirming expression of each gene in the transfected cells.

Fig. 4(a) shows an overlay image of differential interference contrast microscopy (DIC) and EGFP fluorescence, where Ca++ imaging was conducted. Fig. 4(b) shows a representative image of an odorant-evoked Ca++ response when a micropipette locally provided 100 μM BOL at an EGFP positive test cell, *e.g.*, cell #1 in Fig. 4(b). Fig. 4(c) (i) demonstrates that fluorescence transients of Ca++ imaging at the test cell increased up to 0.5 or more with a high reproducibility across trails. On the other hand, no response was found in Fig. 4(c) (ii) when normal BSS buffer was administered. This result indicates that Ca++ responses were evoked by BOL, but not by mechanical stress. At the end of experiments, Ca++ responses to 50 μM glutamate confirmed the survival of this test neuron throughout the experiments, as shown in Fig. 4(c) (iii).

Ca++ transients of other cells, *i.e.*, cells #2–#10 in Fig. 4(b), in addition to the test cell, *i.e.*, cell #1, are depicted in Fig. 4(d). Although these cells except for the test cell were EGFP-negative, they showed synchronous increase of calcium signals at the presentation of BOL at every trial. Thus, neuronal responses at a transfected cell were likely propagated to non-transfected cells *via* synaptic connections.

In Fig. 5, to confirm this possibility of synaptic propagation, Ca++ responses at both EGFP-positive and negative cells were then measured with synapse blockers when BOL was locally administered to EGFP-positive cells. Before applying synapse blockers, both EGFP-positive and negative cells,*i.e.*, cells #1 and #2 in Fig. 5(a), were synchronously activated at the presentation of BOL at every trial [Fig. 5(b) (i)]. With synapse blockers, on the other hand, Ca++ signals of EGFP-negative cells became absent, while EGFP-positive cells still showed clear Ca++ signals [Fig. 5(b) (ii)]. Thus, Ca++ responses at non-transfected cells were elicited by synaptic transmission from odorant-evoked responses at transfected cells.

Lastly, to test how spatiotemporal activity patterns of transfected neuronal cultures depended on stimulus intensity, the entire neuronal culture was perfused with BOL at different concentrations, *i.e.*, 1 μM and 10 μM BOL. Fig. 6(a) and (b) show the test sample and odorant-evoked Ca++ responses to indicated BOL concentrations, respectively. Considering $\Delta F/F >$ 0.2 as odorant-evoked Ca++ responses, 1 μM BOL [Fig. 6(b) (i)] evoked Ca++ responses at 7 cells, *i.e.*, cells #1, 6, 7, 8, 10, 12 and 13 in Fig. 6(a), out of 13 cells, all of which showed activations in response to 10 μM BOL [Fig. 6(b) (ii)]. Fig. 6(c) also demonstrates that fluorescence transients of Ca++ imaging at these labeled cells clearly depend on the BOL concentration. Note that among these labeled cells, only cell #1 was GFP-positive, which presumably activated the negative cells synaptically. These results confirm that the overall activity pattern of a transfected neuronal culture as well as a single transfected cell was dose-dependent.

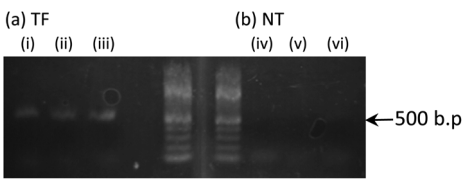

Fig. 3 RT-PCR. (a) Transfected cells (TC); (b) non-trasfected cells (NT): (i), BmOR1; (ii), BmorOrco; (iii), EGFP. The bands at 600 b.p. indicate the presences of mRNA of BmOR1, BmorOrco and EGFP, respectively. Two lanes at the center are size markers.

Discussion

We have provided the proof-of-concept for a novel odorant biosensor, which has ionotropic odorant receptors of insects expressed into a dissociated culture of rat neurons. The simply structured receptors in the insect olfactory system allow easier functional expression than alternative GPCRs. Neuronal culture is an attractive medium in terms of prolonged lifetime and an ability to amplify the weak ionic current of odorant signals into detectable action potentials. In the present work, confocal imaging first confirmed that the odorant receptors were expressed on a membrane of cell [Fig. 2(b)]. Second, fluorescent microscopic observation with the help of immunocytochemistry identified that the co-transfection efficiency of odorant receptors was 8% [Fig. 2(c)]. Third, RT-PCR further confirmed the expression of odorant receptors at the mRNA level (Fig. 3). Lastly, Ca++ imaging demonstrated that the odorant receptors were functionally expressed in neurons and the odor-evoked signals were amplified into spatio-temporal activity patterns in the neuronal culture (Fig. 4–6).

For transfection, lipofection was used in the present study, although the transfection efficiency was lower in lipofection than in viral transfection. The advantages of lipofection over viral transfection are conciseness, quickness, and lower invasiveness.[9] In addition, lipofected sensors can be used anywhere, while viral transfected sensors have to be used in strictly restricted areas.

The transfection efficiency of 8% seemed sufficient for the proposed odorant sensor [Fig. 2(c)]; much higher transfection efficiency should be required when odorant receptors are expressed onto a non-neuronal culture, *e.g.*, HEK-293 cells.[2] In our proposed sensor, even though the efficiency was not very high, the activity of transfected neurons can be amplified into population activities through synaptic connections. In fact, in the present experiments, odorant-evoked synchronous Ca++ transients were found in non-transfected neurons as well as transfected neurons (Fig. 4 and 5). Moreover, Ca++ transients of both transfected and non-transfected neurons changed in a dose-dependent manner (Fig. 6). Thus, the neuronal culture provided an advantageous odorant signal amplification function owing to

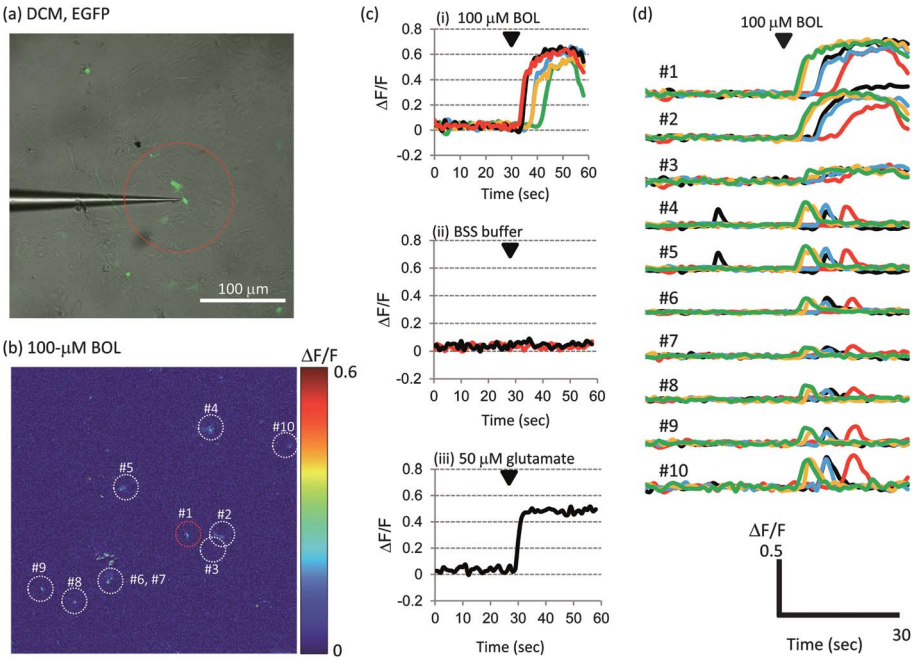

Fig. 4 Ca++ imaging in response to odorant stimulation. (a) Neuronal culture under test. BmOR1, BmorOrco and EGFP were simultaneously co-transfected onto this culture. A differential interference contrast microscopic view (DCM) and EGFP fluorescent view were overlaid. (b) Spatial pattern of Ca++ signal in response to 100 μM bombykol (BOL). Odorant responsive cells (#1–#10) were labeled. BOL was administered to Cell #1 (red circle). Ca++ signals were quantified as fractional changes of fluorescence ($\Delta F/F$). (c) Time courses of Ca++ signal in cell #1. Triangles indicate the time of administration of test substances: (i), 100 μM bombykol (BOL); (ii), BSS; (iii), 50 mM glutamate. Each trajectory is obtained from different trials. (d) Time courses of Ca++ signal in cells #1–#10. Only cell #1 was GFP-positive, while others cells (#2–#10), negative.

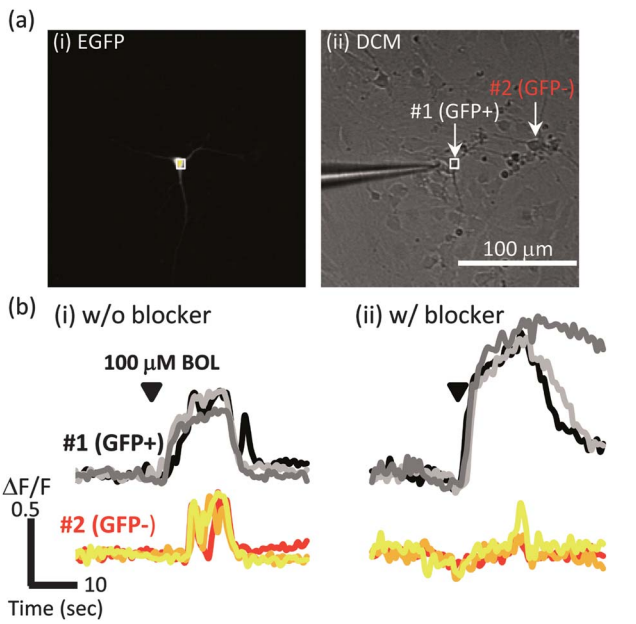

Fig. 5 Synaptic transmission from a transfected cell to non-transfected cells. (a) Test sample: (i), EGFP fluorescence; (ii), light microscopic view. BmOR1, BmorOrco and EGFP were co-transfected onto this sample. Ca++ signals were investigated in Cells #1 and #2, which were GFP-positive and negative, respectively. (b) Time courses of Ca++ signals (i) without and (ii) with synapse blockers. Data from 3 independent trials are overlaid.

a strong cell–network interaction,[18] which has been commonly found in neural networks ranging from dissociate cultures *in vitro*[19–22] to sensorimotor cortices *in vivo*.[23–25]

Co-transfection efficiency of BmOR1 and BmorOrco in sequential transfection was much lower than in simultaneous transfection [Fig. 2(d)]. This low efficiency may be useful when a number of different receptors are expressed in a neuronal culture to develop a multi-odor sensor. That is, sequential transfection could better differentiate receptor expression among cells than simultaneous transfection, thus resulting in more distinct odorant-dependent activity patterns.

The non-linear amplification of odorant signals in neuronal cultures also solves the tradeoff between detection reliability and detection time; the maximal Ca++ signal was observed within 5 s, which is significantly faster than previously reported hybrid odorant biosensors.[1–3] These results indicate the possibility of real-time detection of odorants.

The functioning of the proposed odorant sensor depends on the functional period of odorant receptors as well as the lifetime of neurons. Direct confocal observation in transfected neuronal cells demonstrated that both BmOR1 and BmorOrco were targeted onto a plasma membrane (Fig. 2). However, other receptors are retained in endoplasmic reticulum (ER) and degrade over time unless ER transportation signals are produced, resulting in a limited functional period.[26] Thus, to prolong the functional period of odorant receptors appropriate ER transportation signals have to be identified and introduced.

The lifetime of neurons is expected to be far longer than the functional period of odorant receptors, *i.e.*, as long as the species lifetime, because most neurons do not turn over throughout the

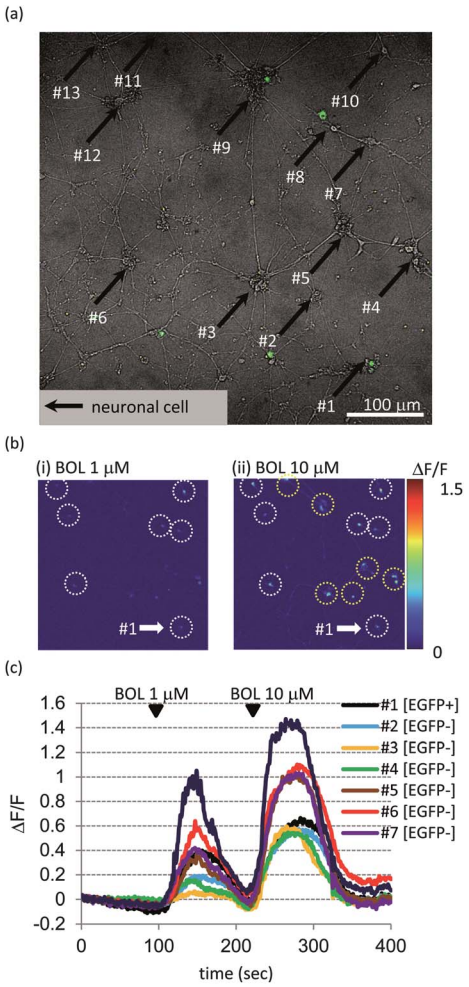

Fig. 6 Dose-dependent spatio-temporal activities of culture. (a) Light microscopic view of test sample. The odorant responsive cells are labeled: #1, transfected cell; #2–#13, non-transfected cells. (b) Spatial pattern of odorant-evoked Ca++ signals: (i) 1 μM BOL; (ii), 10 μM BOL. The location of cell #1, the transfected neuron, is indicated. White circular dots indicate cells responsive (*i.e.*, $\Delta F/F > 0.2$) to both 1 μM and 10 μM BOL. Yellow circular dots indicate cells responsive to only 10 μM BOL but not to 1 μM BOL. (c) Time courses of Ca++ signals of individual neuronal cells. Triangles indicate openings of stopcocks for perfusion of BOL.

species lifetime, a few years for rats. However, invasive measurements such as dye loading for Ca++ imaging should significantly shorten the lifetime. Instead, considering that neurons produce action potentials which are measurable non-invasively and extracellularly, and that non-transfected neurons show odorant-evoked signals, a microelectrode array[19,27,28] is a desirable option for neural measurements in our sensor.

Lastly, plasticity in the neuronal network should be considered during prolonged use. DIV dependent long-term stability and reproducibility of activity patterns after repeated stimuli are important issues to be addressed in future studies.

Conclusion

We have proposed a novel hybrid odorant biosensor by means of expressing ionotropic odorant receptors of insects into dissociated neuronal cultures of rats. This combination of materials brings significant advantages such as easy functional expression, prolonged lifetime, and an ability to amplify the weak ionic currents of odorant receptors. Our experiments have demonstrated that co-transfection efficiency of BmOR1 and BmorOrco was 8%, and both receptors were co-localized on a cell membrane. In Ca++ imaging experiments, synchronous increase of calcium signals at the presentation of BOL was found in both transfected cells and non-transfected cells in a dose-dependent manner. These results provide the proof-of-concept of the proposed odorant sensor.

Acknowledgements

We thank Dr Shigeru Matsuyama at Tsukuba University for bombykol, and Dr Mitsuhiro Morita at Kobe University for pEF-EGFP. This work was partially supported by KAKENHI (23656174) and Nakatani Foundation.

References

1 Q. Liu, W. Ye, L. Xiao, L. Du, N. Hu and P. Wang, *Biosens. Bioelectron.*, 2010, **25**, 2122–2127.
2 H. Ko and T. Park, *Biosens. Bioelectron.*, 2005, **20**, 1327–1332.
3 N. Misawa, H. Mistuno, R. Kanzaki and S. Takeuchi, *Proc. Natl. Acad. Sci. U. S. A.*, 2011, **107**, 15340–15344.
4 C. Wu, P. Chen, H. Yu, Q. Liu, X. Zong, H. Cai and P. Wang, *Biosens. Bioelectron.*, 2009, **24**, 1498–1502.
5 S. Ling, T. Gao, J. Liu, Y. Li, J. Zhou, J. Li, C. Zhou, C. Tu, F. Han and X. Ye, *Biosens. Bioelectron.*, 2010, **26**, 1124–1128.
6 Q. Liu, N. Hu, W. Ye, H. Cai, F. Zhang and P. Wang, *Biosens. Bioelectron.*, 2011, **27**, 12–17.
7 K. Sato, M. Pellegrino, T. Nakagawa, T. Nakagawa, L. Vosshall and K. Touhara, *Nature*, 2008, **452**, 1002–1006.
8 S. Potter and T. Demarse, *J. Neurosci. Methods*, 2001, **110**, 17–24.
9 P. L. Felgner, T. R. Gadek, M. Holm, R. Roman, H. W. Chan, M. Wenz, J. P. Northrop, G. M. Rihgold and Danielsen, *Proc. Natl. Acad. Sci. U. S. A.*, 1987, **84**, 7413–7417.
10 T. Sakurai, T. Nakagawa, H. Mitsuno, H. Mori and Y. Endo, *Proc. Natl. Acad. Sci. U. S. A.*, 2004, **101**, 16653–16658.
11 T. Nakagawa, T. Sakurai, T. Nishioka and K. Touhara, *Science*, 2005, **307**, 1638–1642.
12 J. Krieger, O. Klink, C. Mohl, K. Raming and H. Breer, *J. Comp. Physiol.*, 2003, **189**, 519–526.
13 L. B. Vosshall and B. S. Hansson, *Chem. Senses*, 2011, **36**, 497–498.
14 J. Suzurikawa, H. Takahashi, R. Kanzaki, M. Nakao, Y. Takayama and Y. Jimbo, *Appl. Phys. Lett.*, 2007, **90**, 093901.
15 J. Suzurikawa, M. Nakao, Y. Jimbo, R. Kanzaki and H. Takahashi, *IEEE Trans. Biomed. Eng.*, 2009, **56**, 2660–2665.
16 S. Potter and T. DeMarse, *J. Neurosci. Methods*, 2001, **110**, 17–24.
17 R. Tsuchuya, F. Yoshiki, Y. Kudo and M. Morita, *Brain Res.*, 2002, **956**, 221–229.
18 J. Wolfe, A. R. Houweling and M. Brecht, *Curr. Opin. Neurobiol.*, 2010, **20**, 306–312.
19 H. Takahashi, T. Sakurai, H. Sakai, D. J. Bakkum, J. Suzurikawa and R. Kanzaki, *BioSystems*, 2012, **107**, 106–112.
20 R. Miles and R. K. S. Wong, *Nature*, 1983, **306**, 371–373.
21 L. M. de la Prida, G. Huberfeld, I. Cohen and R. Miles, *Neuron*, 2006, **49**, 131–142.
22 Y. Jimbo, A. Kawana, P. Parodi and V. Torre, *Biol. Cybern.*, 2000, **83**, 1–20.
23 A. R. Howeling and M. Brecht, *Nature*, 2008, **451**, 65–68.
24 M. Brecht, M. Schneider, B. Sakmann and T. W. Margrie, *Nature*, 2004, **427**, 704–710.
25 M. London, A. Roth, L. Beeren, M. Hausser and P. Latham, *Nature*, 2010, **466**, 466–472.
26 M. Lu, F. Echeverri and B. Moyer, *Traffic*, 2003, **4**, 416–433.
27 I. Baruchi and E. Ben-Jacob, *Phys. Rev. E: Stat., Nonlinear, Soft Matter Phys.*, 2007, **75**, 050901.
28 Y. Jimbo, T. Tateno and H. P. C. Robinson, *Biophys. J.*, 1999, **76**, 670–678.

